

## 26.2 Single-Inductor Dual-Input Dual-Output Buck-Boost Fuel-Cell-Li-Ion Charging DC-DC Converter Supply

Suhwan Kim, Gabriel A. Rincón-Mora

Georgia Institute of Technology, Atlanta, GA

Self-powered wireless micro-sensors and other miniaturized wireless systems provide energy-saving and performance-enhancing intelligence to state-of-the-art biomedical and consumer electronics and difficult-to-replace technologies such as power grids and manufacturing plants. Unfortunately, micro-scale dimensions constrain energy (i.e., lifetime) and power (i.e., functionality), and wireless micro-sensors require both: for extended sense/stand-by periods and transmission. These applications exhibit high peak-to-average-power ratios, however, given that transmission demands considerably more power than processing sensory inputs, peak-power and energy requirements are normally mutually exclusive, which is why complementing a power-dense source like the Li-ion battery with its energy-dense counterpart like the fuel cell (FC) improves micro-scale integration and performance [1].

Managing a hybrid micro-source to supply power to a load also demands a power- and space-efficient supply circuit. In this respect, although linear regulators are relatively simpler, faster, and less noisy, switching converters are generally more power efficient, because the voltages across the switches in the power path are in mV range, and consequently more appealing. Using only one inductor as a time-multiplexed transfer medium is also important because printed-circuit board real estate is a precious commodity [2].

As a result, buck or boost single-inductor dual-input dual-output (SIDIDO) converters are popular in power-management [3] and energy-harvesting [4] applications. The foregoing FC-Li-ion hybrid, as shown in Fig. 26.2.1 and unlike most applications discussed in literature, draws energy and power from a 0.6V FC and a 2.7-to-4.2V Li-ion battery to supply a 1V load and recharge the Li-ion battery, when unloaded, requiring a buck-boost charger-supply circuit. To this end, this paper describes and discusses the experimental results of the SIDIDO first introduced in [5].

The converter (Fig. 26.2.1) transfers energy from the FC and Li-ion battery to load  $I_{LOAD}$  (i.e., sensor, transmitter, etc.) and from the FC to the Li-ion battery by energizing and de-energizing inductor L in alternate cycles and phases. The FC, for example, energizes L via switches  $S_1$  and  $S_{E2}$  in one cycle, and  $S_1$  and  $S_0$  de-energize L into  $I_{LOAD}$  in another, and  $S_1$  and  $S_{DE1}$  de-energize L into the Li-ion battery in another phase. Similarly, the Li-ion battery energizes L with  $S_{E1}$  and  $S_0$  in one cycle and  $S_{DE2}$  and  $S_0$  de-energize L into  $I_{LOAD}$  in another. The general strategy is to draw peak power from the Li-ion battery and average power from the FC, recharging the Li-ion with excess FC power during light loading conditions.

The LC tank presents a complex conjugate pole pair to the loop controlling output  $v_o$  so a current loop transforms L into a current source at lower frequencies by regulating the inductor current  $i_L$  at higher frequencies via hysteretic comparator  $CMP_i$ , reducing the pole pair to one pole. Regulating  $i_L$  below 1mA is also important to ensure the FC is neither overloaded or exposed to fast load dumps [6]. A lower bandwidth voltage loop regulates  $v_o$  through hysteretic comparator  $CMP_v$ . From a system perspective, the converter has two modes of operation: light (LT) and heavy (HV). In LT, the FC supplies energy to  $I_{LOAD}$  and the Li-ion battery by regulating  $i_L$  to a value that is slightly above what is necessary to sustain  $I_{LOAD}$  ( $I_{L,REFFC}$ ) so excess energy can be used to recharge the Li-ion. In HV, both the FC and Li-ion battery supply energy to  $I_{LOAD}$  by regulating  $i_L$  to  $I_{L,REFFC}$  when drawn from the FC and to a higher value  $I_{L,REFLI}$  when drawn from the Li-ion. Each mode is comprised of two phases, each relying on burst control to regulate  $v_o$ . In LT, for instance (Fig. 26.2.2(b)),  $C_{OUT}$  charges to the upper hysteretic limit of  $v_o$  when directing FC energy into  $I_{LOAD}$  and discharges to the lower hysteretic limit of  $v_o$  when channeling FC energy to the Li-ion. In HV,  $C_{OUT}$  charges when energy is drawn from the Li-ion battery and discharges when derived from the FC, as the latter supplies less power than  $I_{LOAD}$  demands.

Hysteretic comparator  $CMP_M$  (with a wider hysteresis window than  $CMP_v$ ) controls mode transition by sensing  $v_o$ . As  $I_{LOAD}$  transitions from low to high, the LT energy that the converter supplies is insufficient and therefore  $C_{OUT}$  discharges below  $CMP_v$ 's lower hysteretic limit to  $CMP_M$ 's even lower limit, forcing the system to enter the HV mode and pulling  $v_o$  back to its target. Conversely, when  $I_{LOAD}$  transitions from high to low, the converter's HV energy is excessive so  $C_{OUT}$  charges above  $CMP_v$ 's higher hysteretic limit to  $CMP_M$ 's even higher limit, forcing the circuit back into the LT mode.

In the current-regulation loop, series sense resistors  $R_{S,FC}$  and  $R_{S,LI}$ , as shown in Fig. 26.2.3, sense  $i_L$ . Miller-compensated opamp  $AMP_i$  amplifies  $i_L R_{S,FC}$  and  $i_L R_{S,LI}$  by  $R_{INST,B}/R_{INST,A}$ , and 2-stage comparator  $CMP_i$  ultimately regulates  $i_L$  to its target. The values of  $R_{S,FC}$  and  $R_{S,LI}$  set regulation targets  $I_{L,REFFC}$  and  $I_{L,REFLI}$ , respectively. Using two resistors circumvents the overhead associated with generating two current-setting reference voltages ( $V_{I,REF}$ ). Connecting  $R_{S,FC}$  and  $R_{S,LI}$  to the non-switching side of L, according to the mode and phase of the converter, also relaxes the ICMR requirements attached to  $AMP_i$  (down from rail to rail). Voltage  $V_{OFFSET}$  tunes the average target regulation point of the current loop and current source  $M_{CP5}$  in the positive feedback loop within  $CMP_i$  (along with the delay of the comparator) sets the hysteretic window around which  $i_L$  is regulated. Voltage  $V_{HYS,CTRL}$  is used for testing purposes to eliminate the positive feedback and rely on the comparator delay to set the hysteresis. Figure 26.2.4 illustrates the 2-stage hysteretic comparator used for the voltage and mode-setting loops. The positive feedback gain mirror load  $M_{CN1}-M_{CN4}$  sets the hysteresis window around which  $v_o$  is regulated.

The 0.5 $\mu$ m CMOS controller IC occupies 0.5 $\times$ 1.0mm<sup>2</sup> of silicon area (Fig. 26.2.7) and uses 150 $\mu$ H and 100nF of off-chip inductance and capacitance. The experimental results in Fig. 26.2.5 illustrate how  $i_L$  (via the voltage across the sense resistors) is regulated to (a) 0.9mA, (b) 0.3mA, and (c) 2mA at about 2MHz when drawing energy from (a) the FC to  $I_{LOAD}$ , (b) the FC to the Li-ion battery, and (c) the Li-ion to  $I_{LOAD}$ . The unexpected noise found in the Li-ion- $I_{LOAD}$  phase is attributed to the EMI of inductor and coupled noise through the silicon substrate, both of which are more pronounced during this higher power phase.

Figure 26.2.6 illustrates  $v_o$  during LT and HV modes, when  $I_{LOAD}$  is 0.1mA and 1mA, and in response to 0.1-to-1mA load dumps, for which the converter transitions between modes ( $V_{MODE}$  and  $V_{PHASE}$  indicate the mode and phase of the converter). The voltage loop regulates  $v_o$  in both modes within  $\pm 25$ mV or  $\pm 2.5\%$  of its nominal 1V target and  $\pm 50$ mV during mode transitions. The system transitions automatically, without inadvertent noise-triggered excursions, across modes in response to ascending and descending 0.1-to-1mA load dumps, requiring less than 30 s to recover and regulate  $v_o$  back.

### Acknowledgements:

This work was funded by T&E/S&T through the Naval Undersea Warfare Center (N66604-06-C-2330).

### References:

- [1] R.A. Dougal, S.Liu, and R.E. White, "Power and Life Extension of Battery-Ultracapacitor Hybrids", *IEEE Trans. Components and Packaging Technologies*, vol. 25, no. 1, pp. 120-131, Mar., 2002.
- [2] D. Ma, W.-H. Ki, C.-Y. Tsui, and P.K.T. Mok, "Single-Inductor Multiple-Output Switching Converters with Time-Multiplexing Control in Discontinuous Conduction Mode," *IEEE J. Solid-State Circuits*, vol. 38, no. 1, pp. 89-100, Jan., 2003.
- [3] Y.-H. Lam, W.-H. Ki, C.-Y. Tsui, and P.K.T. Mok, "Single-Inductor Dual-Input Dual-Output Switching Converter for Integrated Battery Charging and Power Regulation," *IEEE International Symp. Circuits and Systems*, vol. 3, pp. 447-450, May, 2003.
- [4] N.-M. Sze, F. Su, Y.-H. Lam, et al., "Integrated Single-Inductor Dual-Input Dual-Output Boost Converter for Energy Harvesting Applications," *IEEE International Symp. Circuits and Systems*, pp. 2218-2221, May, 2008.
- [5] M. Chen and G.A. Rincón-Mora, "Single Inductor, Multiple Input, Multiple Output (SIMIMO) Power Mixer-Charger-Supply System," *International Symp. Low Power Electronics and Design*, pp. 310-315, Aug., 2007.
- [6] C.W. Moore, J. Li, and P.A. Kohl, "Microfabricated fuel cells with thin-film silicon dioxide proton exchange membranes," *Journal of the Electrochemical Society*, vol. 152, no. 8, pp. A1606-1612, Aug., 2005.

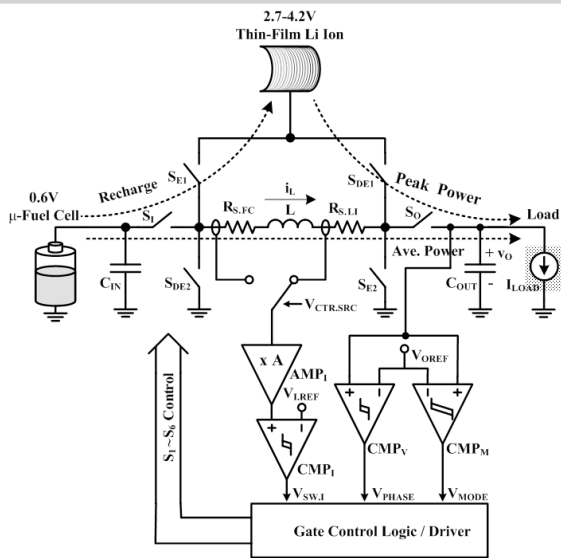


Figure 26.2.1: FC-Li-ion charger-supply circuit.

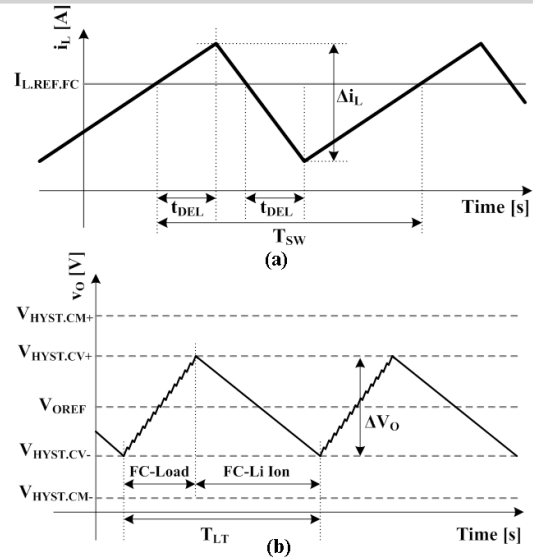


Figure 26.2.2:  $i_L$  and  $v_O$  graphs under light load.

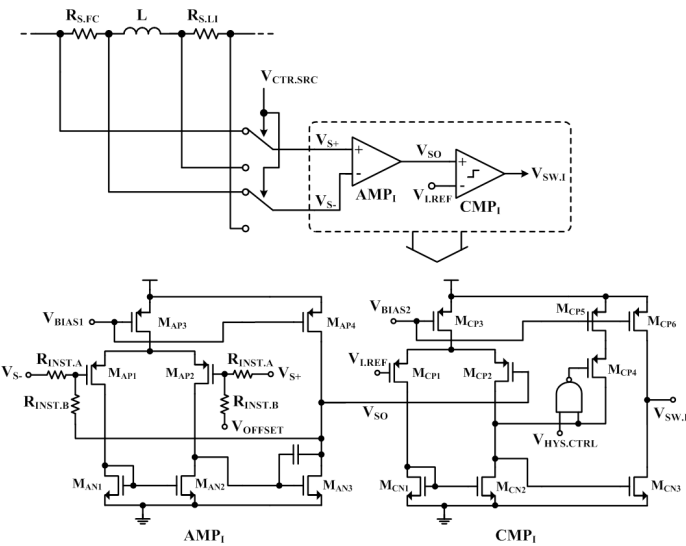


Figure 26.2.3: Current-regulation path.

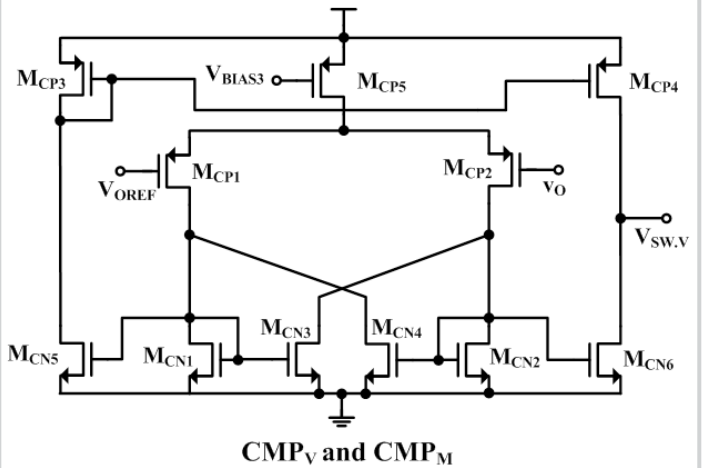


Figure 26.2.4: Voltage- and mode-regulation comparator.

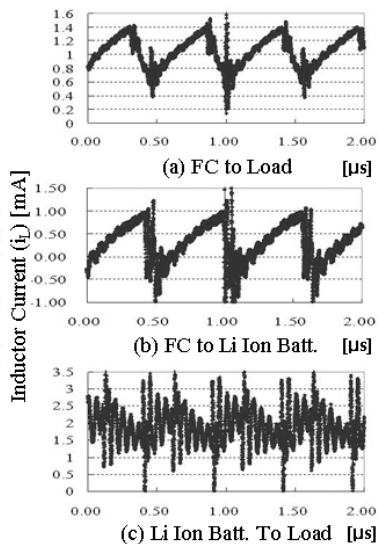


Figure 26.2.5: Experimental  $i_L$  regulation results.

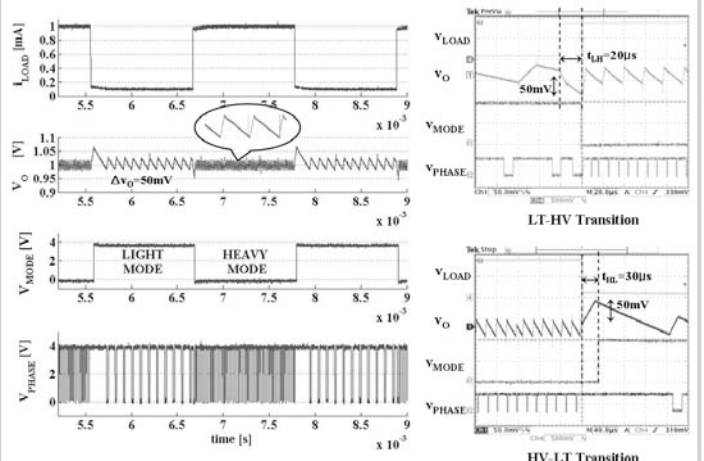


Figure 26.2.6: Experimental  $v_O$  regulation results.

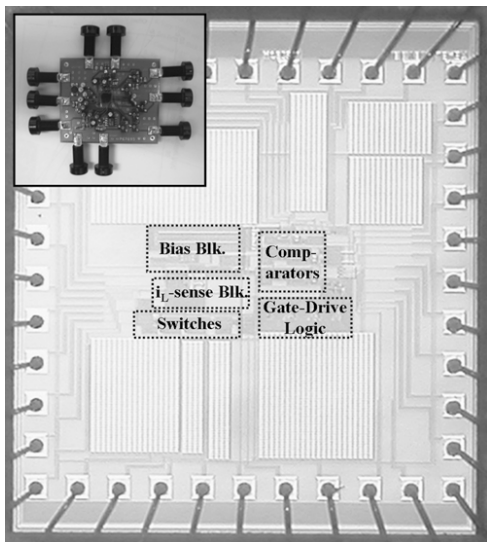


Figure 26.2.7: Chip micrograph and evaluation PCB.